Available online at www.sciencedirect.com
SCIENCE DIRECT
Journal of Molecular Catalysis A: Chemical 250 (2006) 169–176
JOURNAL OF MOLECULAR CATALYSIS A: CHEMICAL
www.elsevier.com/locate/molcata

Structural and catalytic investigation of vanadia supported on ceria promoted with high surface area rice husk silica

T. Radhika, S. Sugunan *

Department of Applied Chemistry, Cochin University of Science and Technology, Cochin-22, Kerala, India

Received 23 September 2005; received in revised form 13 January 2006; accepted 24 January 2006
Available online 3 March 2006

Abstract

Rice husk silica was utilized as the promoter of ceria for preparing supported vanadia catalysts. Effect of vanadium content was investigated with 2–10 wt.% V_2O_5 loading over the support. Structural characterization of the catalysts was done by various techniques like energy dispersive X-ray (EDX), X-ray diffraction (XRD), BET surface area, thermal analysis (TGA/DTA), FT-infrared spectroscopy (FT-IR), UV–vis diffused reflectance spectroscopy (DR UV–vis), electron paramagnetic spectroscopy (EPR) and solid state magnetic resonance spectroscopies (^{29}Si and ^{51}V MASNMR). Catalytic activity was studied towards liquid-phase oxidation of benzene. Surface area of ceria enhanced upon rice husk silica promotion, thus makes dispersion of the active sites of vanadia easier. Highly dispersed vanadia was found for low V_2O_5 loading and formation of cerium orthovanadate ($CeVO_4$) occurs as the loading increases. Spectroscopic investigation clearly confirms the formation of $CeVO_4$ phase at higher loadings of V_2O_5. The oxidation activity increases with vanadia loading up to 8 wt.% V_2O_5, and further increase reduces the conversion rate. Selective formation of phenol can be attributed to the presence of highly dispersed active sites of vanadia over the support.
© 2006 Elsevier B.V. All rights reserved.

Keywords: Supported vanadia; Rice husk silica; $CeVO_4$; NMR; EPR; Benzene oxidation

1. Introduction

Vanadia containing catalysts probably constitute the family of catalysts often used for partial oxidation of organic compounds and selective oxidation with rupture of C–C bond [1–3]. Generally, bulk V_2O_5 cannot be used as a catalyst because of its poor thermal stability and mechanical strength. Therefore, vanadia is normally supported on different carriers depending on the type of the reaction to be catalyzed [4–6]. It has been observed that the selectivity and activity of these catalysts depend on, among other factors, the vanadium loading, the method of support, state of vanadia in the support, calcination temperatures, type of support and its surface acidity [7,8]. A better understanding of the catalytic properties of supported vanadia requires determination of the structure–reactivity relationships of the supported vanadia catalysts. As a consequence, considerable attention has been focused on the preparation, characterization and evaluation of vanadium oxide catalysts deposited on various single as well as on mixed oxides. Silica is a well known support and the application of silica as a catalyst support has been extensively studied to meet the demand for high melting point, high metal dispersion, higher thermal stability and surface area and consequently high activity [9,10]. The catalytic efficiency of ceria is based on the oxygen storage and diffusion through lattice defects in CeO_{2-x}. The Ce^{4+}/Ce^{3+} redox couple in ceria containing catalysts is known to be responsible for this intrinsic property [11,12]. This oxide is one of the most important components of fluid catalytic cracking (FCC) and three way catalysts (TWC) [13]. CeO_2 is frequently incorporated into oxidation catalysts because it shows a considerable performance for the catalytic combustion of hydrocarbons and various gaseous pollutants. Recent studies have suggested that formation of mixed oxides of ceria enhances the catalytic, textural, redox and oxygen storage properties of ceria and the oxide catalysts so-formed also exhibit good thermal stability [14].

Rice husk is one of the byproducts of rice, a major food material of most of the developing countries including India. The partially burnt rice husk in turn contributes to more environmental pollution and is an abundant waste material in all rice producing countries [15]. The presence of silica in rice husk has

* Corresponding author. Tel.: +91 484 2575804; fax: +91 484 2577595.
E-mail address: ssg@cusat.ac.in (S. Sugunan).

1381-1169/$ – see front matter © 2006 Elsevier B.V. All rights reserved.
doi:10.1016/j.molcata.2006.01.048

been known since 1938. Rice husk on burning gives ash containing >90% silica, which is normally in the crystalline form [16]. However, under controlled burning conditions it gives amorphous silica, which is highly reactive due to its ultrafine size and high surface area [17]. Instead of the silica gel (SiO_2) commonly used, rice husk ash has been first adopted as a catalyst support by Chang et al. and found to exhibit a very high activity for the rice husk ash supported nickel catalysts in CO_2 hydrogenation [18]. Consequently, preparation of catalysts utilizing rice husk silica, which is composed of pure amorphous silica, is very attractive [19–21]. Present work describes the preparation of vanadia catalysts supported on ceria promoted with rice husk silica and were characterized in detail using different instrumental techniques. Catalytic activity was tested using liquid-phase oxidation of benzene.

2. Experimental

2.1. Catalyst preparation

The rice husk (Rice mill, Cochin, Kerala) was first washed with distilled water to remove adhering materials and dried. It was leached with 10% solution of HCl in distilled water at its boiling point for 3 h. The digested husk was then washed with distilled water and dried in an oven at 110 °C for 12 h. Pure amorphous white silica (RS) was obtained by burning this rice husk at 600 °C in a muffle furnace for 6 h. Ceria (CeO_2) was prepared via hydroxide method with 1:1 NH_3 solution (NH_3:distilled water/ml) under mechanical stirring from $Ce(NO_3)_3{\cdot}6H_2O$ (IRE, Udyogamandal, Kerala) at pH 10–11. Rice husk silica promoted ceria (CRS, 1:1 mole ratio based on oxides) was prepared by deposition precipitation method in which, requisite quantities of $Ce(NO_3)_3{\cdot}6H_2O$ and silica were mixed together and precipitated by NH_3. Supported vanadia catalysts were prepared by wet impregnation method. To impregnate vanadia, the requisite quantity of ammonium metavanadate (CDH, LR) was dissolved (0.001 M)in aqueous oxalic acid solution (0.1 M) and to this clear solution, dried support was added and mechanically stirred for 6 h. After keeping overnight the excess water was evaporated. The hydroxides were oven dried at 110 °C for 12 h and sieved to mesh size below 100 μm. Calcination of the catalysts was carried out for 5 h in a closed muffle furnace in flowing air prior to use. Catalysts are denoted as xVCRS where $x = 2$, 4, 6, 8 and 10 wt.% V_2O_5 and VCRS for V_2O_5/CeO_2-rice husk silica.

2.2. Characterization

The chemical composition of catalysts was obtained from Stereoscan 440 Cambridge, UK energy dispersive X-ray analyzer used in conjunction with SEM. Powder X-ray diffraction pattern was collected using Rigaku D-Max Ni filtered Cu Kα radiation. Micromeritics Flow Prep-060 Gemini 2360 instrument was used to determine the BET surface area and total pore volume with N_2 adsorption at 77 K. TGA/DTA were collected on a Perkin Elmer Pyris Diamond thermogravimetric/differential thermal analyzer instrument under nitrogen atmosphere at heating rate of 20 °C/min from room temperature to 800 °C with samples mounted on an alumina sample holder. Infrared spectra were obtained by the KBr technique over the wavenumber range 400–4000 cm^{-1} by using ABB BOMEM (MB Series) FT-IR spectrophotometer. DR UV–vis spectra were taken in the range 200–800 nm with MgO as reference using Ocean Optics, Inc. SD 2000, Fiber Optic Spectrometer with a charged coupled device detector. The EPR experiments were conducted at X-band at room temperature. Solid-state ^{29}Si and ^{51}V MASNMR spectra were collected over a Bruker DSX-300 spectrometer with a standard 4 mm double bearing Bruker MAS probe. Isotropic chemical shifts were reported relative to neat NH_4VO_3. The solid-state ^{51}V MASNMR spectra of catalysts calcined at 500 °C were recorded with a spinning frequency $\nu_R = 7.0$ kHz.

2.3. Liquid-phase oxidation of benzene

Oxidation of benzene was conducted in a 50 ml round bottom flask stirred with a magnetic stirrer which was connected to a condenser and immersed into a thermo stated oil bath, where it was maintained for the reaction time of 6 h. The solvent acetonitrile (191 mmol), benzene (11 mmol) and catalyst (100 mg) were added to the flask in that order and oxidant 30% H_2O_2 (88 mmol) after attaining the reaction temperature (60 °C). The reaction products were analyzed by Chemito GC 1000 gas chromatograph equipped with flame ionization detector containing BP-1 capillary column. Conversion and selectivity were calculated compared with relative area of each of authentic samples. Analysis condition was programmed from 60 °C-3 min-20°/min to 280 °C with injection and detection temperature of 200 °C.

3. Results

3.1. Physico-chemical characterization

Chemical composition, BET surface area measurements and the crystallite size calculated by Scherrer formula from XRD data are shown in Table 1. Silica prepared contains 98.81% Si with traces of Na. The EDX analysis shows that amount of V (at.%) on the support increases upon increase in wt.% V_2O_5 loading. High purity silica with BET specific surface area 224 $m^2\,g^{-1}$ could be obtained from rice husk. Upon silica promotion the surface area of ceria have been increased from 67 to 102 $m^2\,g^{-1}$. Increase in pore volume also observed with corresponding reduction in crystallite size. Incorporation of V_2O_5 leads to a consistent decrease in the specific surface area and such a decrease is more pronounced as the vanadium content increased. This is a general phenomenon of supported catalysts, where the surface area of the support decreases with increasing the quantity of the active component up to monolayer coverage of the impregnated one [22]. The decrease in surface area as a function of vanadia content must be attributed to the penetration of the active component into the pores of the support in effect, results high dispersion of the active component on the support. Results suggest that during impregnation and further calcination, strong interaction with the support is developed, leading to

Table 1
Chemical composition and physical properties

Catalysts	Composition (at.%)			BET surface area ($m^2\ g^{-1}$)	Pore volume ($cm^3\ g^{-1}$)	Crystallite size (nm)
	Ce	Si	V			
CeO_2	100	–	–	67	0.11	12
RS	–	98.81	–	224	0.28	–
CRS	55.18	44.82	–	102	0.27	10
2VCRS	39.06	54.88	6.09	94	0.26	8
4VCRS	41.32	52.34	6.34	90	0.25	9
6VCRS	38.29	53.43	8.28	76	0.18	11
8VCRS	43.67	44.79	11.25	66	0.14	12
10VCRS	43.02	40.29	16.70	52	0.15	10

phase interaction of the two metal oxides. However, the extent of decrease in surface area is lower in supported vanadia catalysts, suggesting that the degree of sintering can be reduced with high surface area support in amorphous form. The presence of high surface area support does stabilize small particles and its growth is inhibited usually in a purely mechanical fashion [23].

The X-ray diffraction pattern of rice silica, ceria and supported catalysts calcined at 500 °C are shown in Fig. 1(a). The X-ray reflections of ceria are observed at 2θ ~28.32°, 32.86°, 47.34° and 56.12° corresponding to Miller indices of 1 1 1, 2 0 0, 2 2 0 and 3 1 1, respectively. This shows a typical cubic crystal structure of fluorite type ceria [24]. Silica obtained from rice husk is found to be X-ray amorphous with a broad diffraction peak around 2θ ~22° [25]. As can be seen from the figure, the silica promoted ceria exhibits poor crystallinity with the diffraction lines due to only ceria is visible. The X-ray diffraction patterns of the supported catalysts calcined at two different temperatures are shown in Fig. 1(b) and (c). For catalysts calcined at 500 °C, the intensity of diffraction peaks is found to be low confirming the amorphous nature of CRS support with no appreciable changes in the shape and position of the lines due to CeO_2. However, for 10VCRS calcined at 650 °C in addition to sharp CeO_2 lines, new lines with less intensity is also appeared. But no lines corresponding to V_2O_5 crystallites are observed. The observed new lines can be attributed to the formation of $CeVO_4$. The silica features are not observed since this is in amorphous form and the preferential formation of $CeVO_4$ indicates that supported vanadia interacts selectively with the ceria portion of the promoted support [26]. Similar studies with low surface area metal oxide supports suggest the formation of $CeVO_4$ and further crystallization even at 500 °C [27]. Crystallite size (Table 1) of silica promoted ceria is lowered compared to ceria. For supported vanadia catalysts, a small increase in crystallite size of ceria is observed as the weight percentage of vanadia loading increases. Results suggesting a highly dispersed or amorphous form of vanadium oxide formed on the high surface area silica promoted ceria support. Ceria surface can strongly interact with vanadia species as the V_2O_5 density increases to form $CeVO_4$, in which cerium is reduced from Ce^{IV} to Ce^{III}, whereas the vanadium remains in the +5 oxidation state [28]. Formation of $CeVO_4$ is occurs due to the following reaction:

$$V_2O_5 + 2CeO_2 \rightarrow\ 2CeVO_4 + 1/2O_2$$

Fig. 2 illustrates the TGA/DTA analysis of catalysts conducted before calcination. An endothermic peak observed from room temperature to 200 °C for supported catalysts can be attributed to the removal of water [12]. A second weight loss observed from 300 to 450 °C depending on the catalysts. This can be attributed to the decomposition of oxalates of vanadium and cerium formed during the preparation of supported vanadia catalysts [29,30]. Small endotherm at 700 °C is corresponding to the melting of V_2O_5, since the formation reaction of $CeVO_4$ taking place [31].

The DR UV–vis spectra of the calcined catalysts are shown in Fig. 3. The strong absorption observed in the region 200–400 nm must be assigned to O–Ce charge transfer transitions involving a number of surface Ce^{4+} ions along with O^{2-} to V^{5+} charge transfer transitions for supported catalysts. Catalysts with higher wt.% V_2O_5 loading exhibit a much broader absorption band in the UV region and the absorption tail extends into visible region. This is consistent with the growth in crystallite size and change of coordination structure as more V_2O_5 is deposited on the support surface [32]. Thus, the DR UV–vis spectra imply that highly dispersed tetrahedral VO_4 (V^{5+}) species are present on the support surface for low loading. However, broadening of spectra above 6 wt.% V_2O_5 suggests different vanadia coordination may be due to the formation of $CeVO_4$. The d–d transition, which are typical for reduced vanadium species, are not observed [33].

FT-IR absorption spectra observed are shown in Fig. 4. In the 1000–4000 cm^{-1} region, catalysts showed a broad absorption at 3760–2600 cm^{-1} and a sharp band at 1620 cm^{-1}, due to surface hydroxyls and coordinated water. The band around ~1090 cm^{-1} corresponds to the stretching vibrations of Si–O–Si bond. In supported catalysts, the vibration near ~797 cm^{-1} is attributed to the coupled vibrations of V=O bonds [34].

The EPR spectra of the catalysts are shown in Fig. 5 and the Hamiltonian parameters are listed in Table 2. Signals observed for CeO_2 and g values calculated (f^1 ions: $g_e > g_\perp > g_{||}$) are attributed to the presence of two different types of Ce^{3+} ions. Signal A is due to Ce^{3+} species with removable ligands and signal B is with Ce^{3+} ions stabilized by some lattice defects located in distorted sites of the fluorite structure [35]. Silica promotion reduces the intensity of Ce^{3+} species and only signal B is observed suggesting some interaction between ceria surface and silica. After impregnation of vanadia, intensity of Ce^{3+} species is reduced with only B signal for 2 wt.% V_2O_5 load-

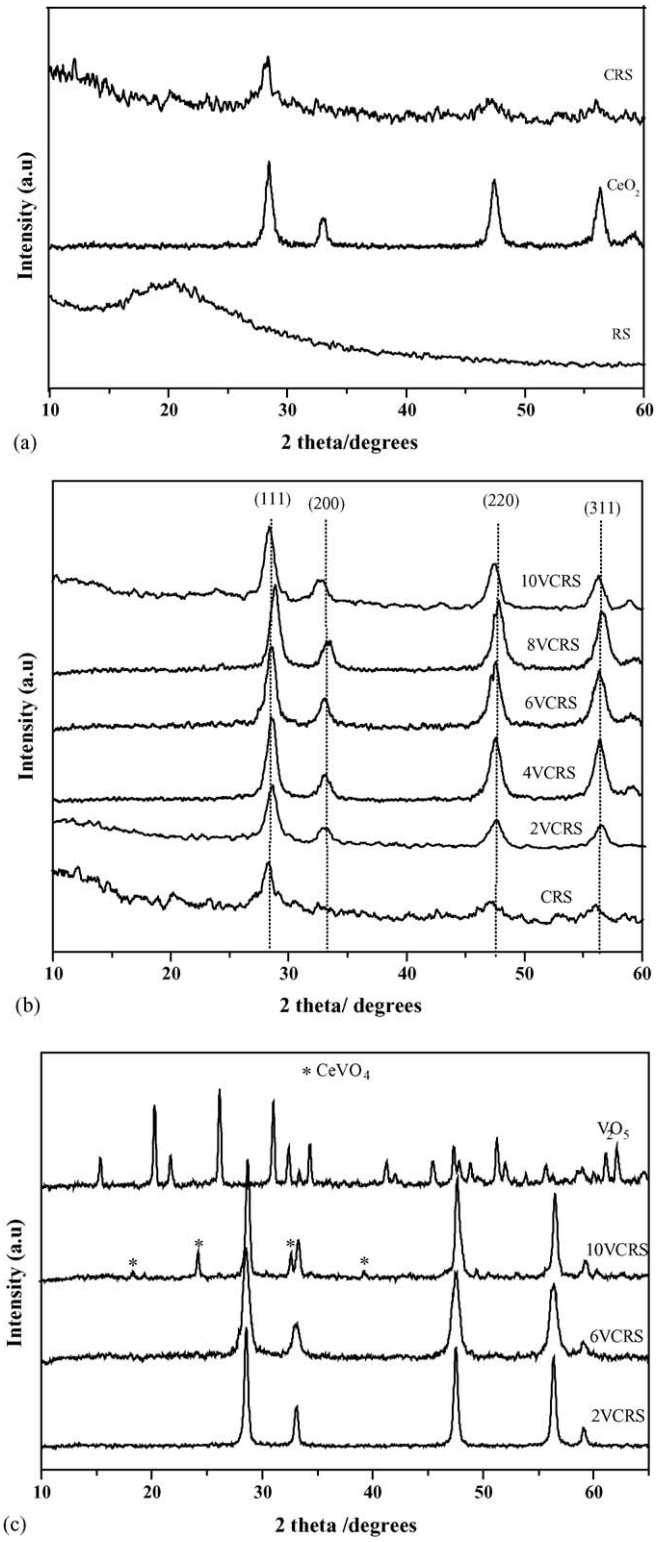

Fig. 1. X-ray diffraction pattern of (a) CeO_2, RS and CRS; (b) VCRS catalysts calcined at 500 °C; (c) VCRS catalysts calcined at 650 °C.

ing, while some new signals observed as the vanadia loading increases. The observance of these signals suggests that presence of vanadia stabilizes the Ce^{3+} species even at high vanadia loading with another new phase formation. Reduction in Ce^{3+} intensity can be explained by the consumption of CeO_2 for the

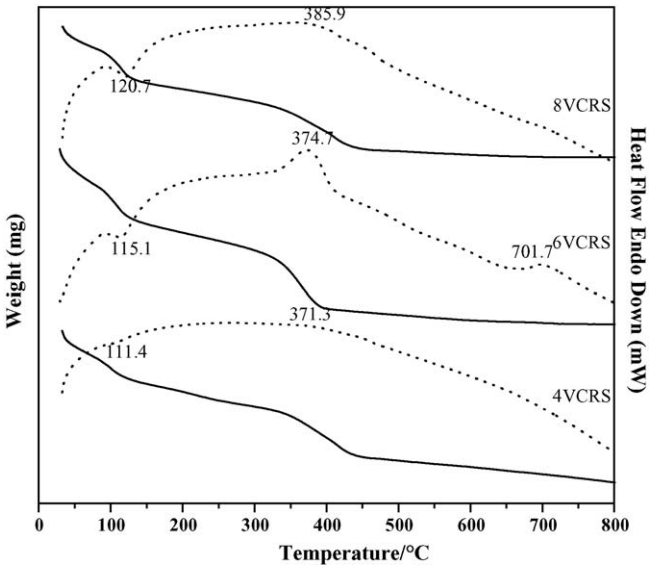

Fig. 2. TGA/DTA pattern of VCRS catalysts.

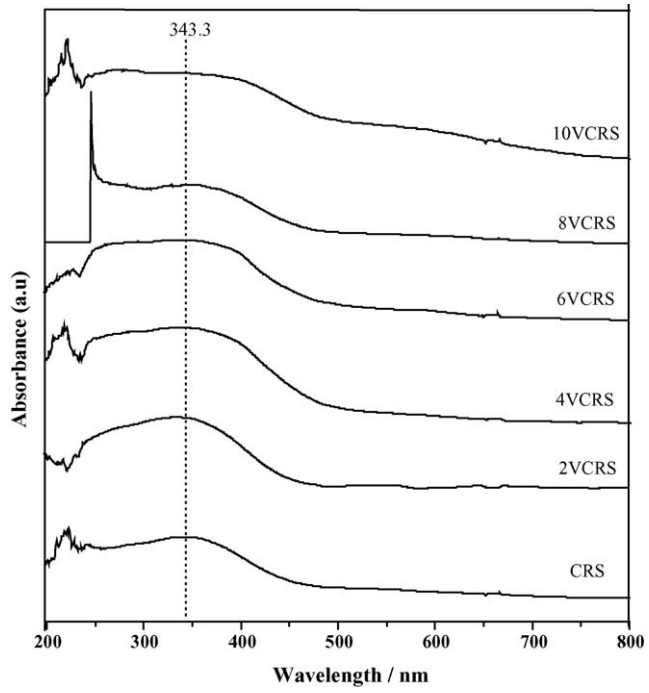

Fig. 3. DR UV–vis spectra of CRS and VCRS catalysts.

Table 2
Spin Hamiltonian parameters

Catalysts	Parameters		
	$g_\perp$	$g_{\|\|}A$	$g_{\|\|}B$
CeO_2	1.966	1.943	1.934
CRS	1.960	–	1.931
2VCRS	1.966	–	1.939
6VCRS	1.984	–	1.949
10VCRS	1.978	–	1.948

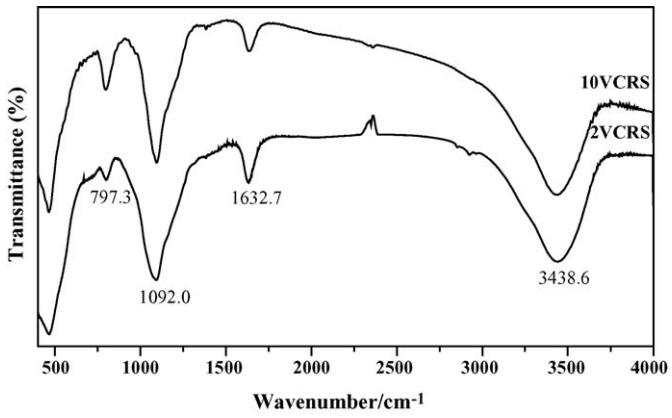

Fig. 4. FT-IR spectra of VCRS catalysts.

formation of $CeVO_4$ over the support for high vanadia loading thus decreasing the concentration. A new signal S observed for 6VCRS and 10VCRS is corresponds to the presence of $CeVO_4$ phase. The observed *g* values for 6VCRS and 10VCRS, suggests vanadia sites in a distorted octahedral coordination [28].

Solid-state NMR methods represent a novel and promising approach to the characterization of supported catalytic materials [36]. ^{29}Si MASNMR spectra of as-prepared catalysts are shown in Fig. 6. The spectra of rice husk silica exhibits shift at −109 ppm and this must be assigned to Q^4, Si $(OSi)_4$ units [37]. In CRS, the broadening of peaks suggests the interaction of silica surface by ceria. In supported catalysts also, bands suggest presence of Q^4 units without any compound formation of Si atoms. This supports the resulting formation of $CeVO_4$ selectively over the support shown from X-ray diffraction. Fig. 7 illustrates ^{51}V MASNMR spectra of samples calcined at 500 °C recorded with spinning frequency 7.8 kHz. At low vanadium content, the spectrum consists of intense bands at −260, −379 and −496 ppm associated with several spinning side bands. The broad line pattern associated with this species could be correlated with an absence of regular ordering of these vanadia sites. The shift at −260 ppm is assigned to the surface vanadium–oxygen structures surrounded by a distorted octahedron of oxygen atoms [38]. The resonance appears at −360 and −495 ppm can be assigned to pseudo-octahedrally coordinated V^{5+} species as a consequence of the interaction of tetrahedral sites and distorted isolated tetrahedral V^{5+} sites, respectively [39]. For low wt.% V_2O_5 loaded catalysts, the species are consistent with surface V=O species highly dispersed on the ceria surface. In the spectra of 6VCRS, a signal centered at −432 ppm has been obtained along with other signals. The chemical shift value around −432 ppm corresponds to the tetragonal structure of $CeVO_4$, in which vanadium atoms are located at the center of isolated tetrahedra [40]. Thus 6 and 8 wt.% V_2O_5 over the support contains highly dispersed tetrahedral vanadium together with $CeVO_4$. For 10VCRS, highly symmetrical signal centered at −433 ppm suggests complete formation of $CeVO_4$ compared to lower vanadia loading.

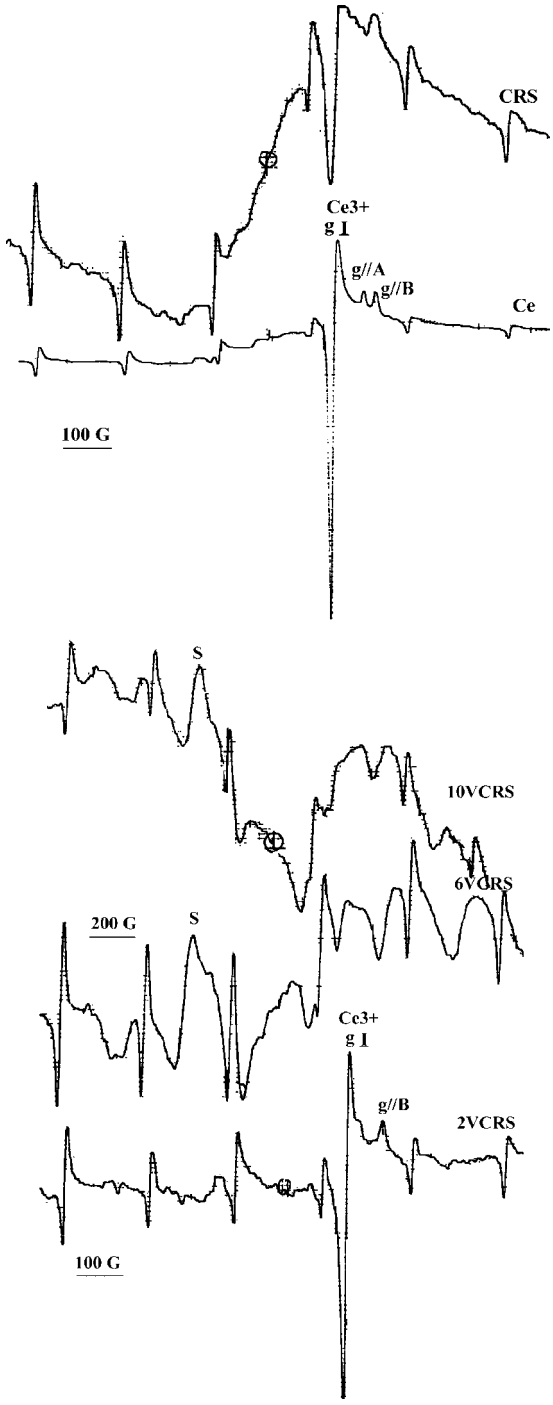

Fig. 5. EPR spectra of CeO_2, CRS and VCRS catalysts.

3.2. Catalytic activity

Table 3 shows data of the liquid-phase oxidation of benzene over the catalysts. H_2O_2 is used as the oxidant since it produces water as the only byproduct. Temperature above 80 °C causes decomposition of H_2O_2 thus usually conversion rate decreases and it is always desirable to select low reaction temperature. Therefore, in present case, the oxidation of benzene conducted at 60 °C in acetonitrile with H_2O_2 as the oxidant. No oxidation occurs when the reaction is carried out with ceria, silica and

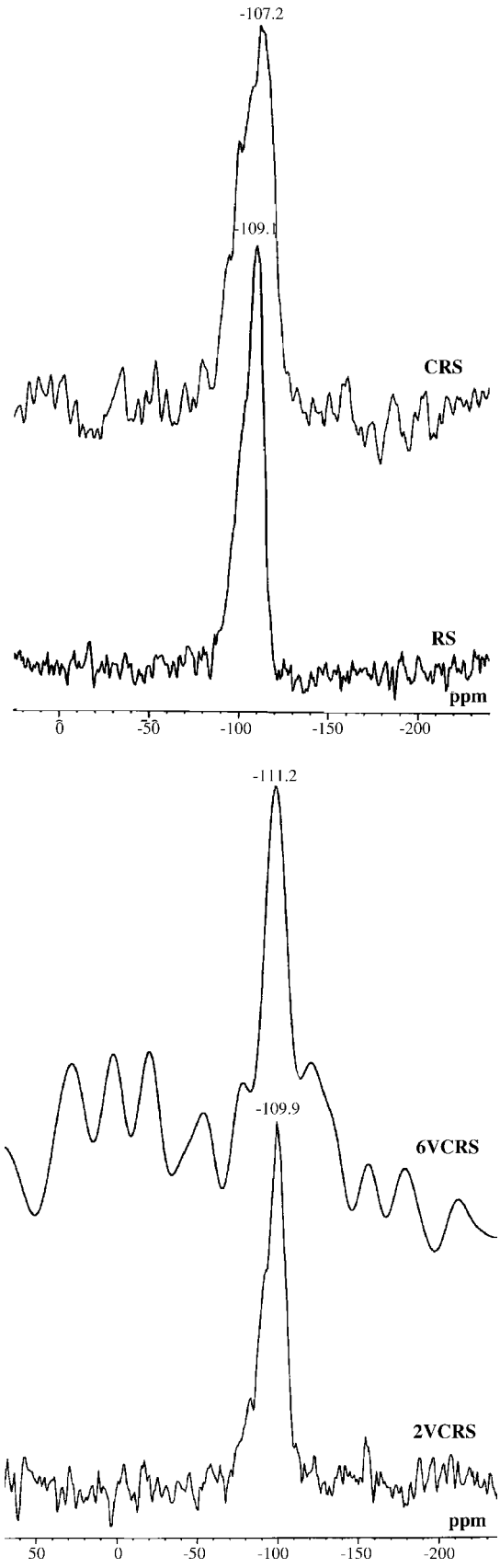

Fig. 6. ^{29}Si MAS NMR spectra of RS, CRS and VCRS catalysts.

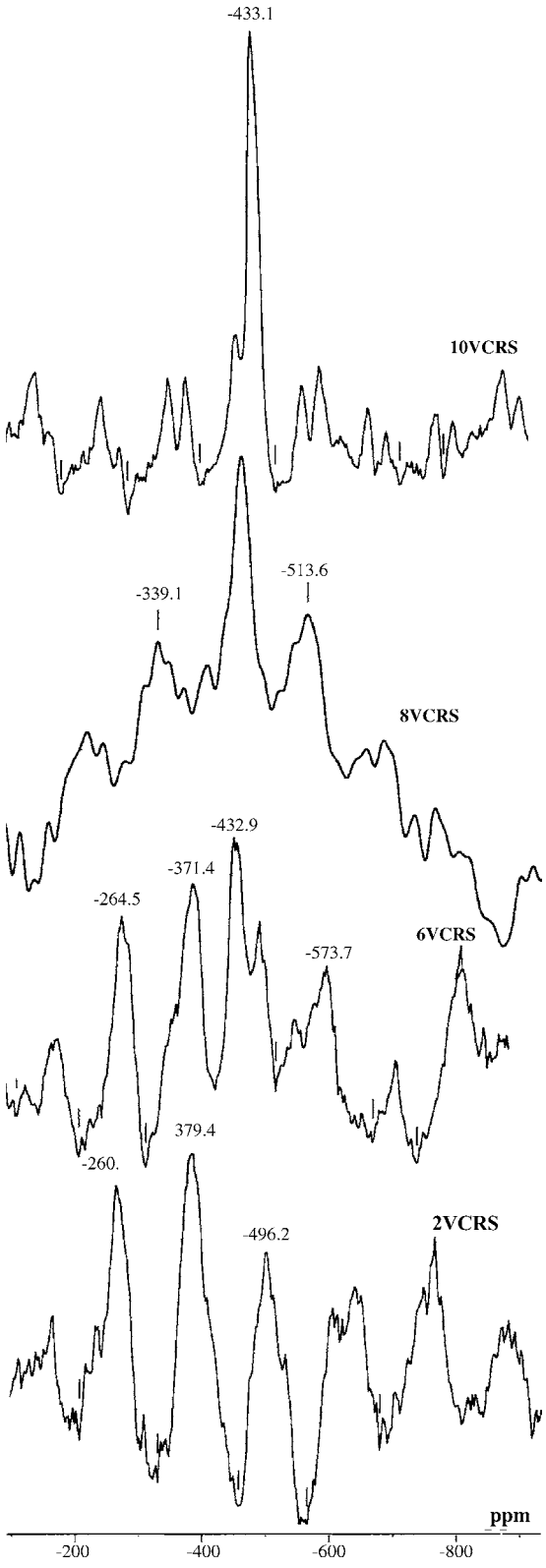

Fig. 7. ^{51}V MAS NMR spectra of VCRS catalysts.

CRS at the set conditions. In the absence of vanadium, ceria is found inactive towards the oxidation of benzene. Results show that upon the addition of vanadium, oxidation took place and phenol was obtained as the only product. Activity increases with increase in vanadia loading up to 8 wt.% V_2O_5. However, further

Table 3
Catalytic performance in benzene oxidation

Catalyst	Conversion (wt.%)	Phenol (%)
CeO_2	–	–
CRS	–	–
2VCRS	2.8	100
4VCRS	7.9	100
6VCRS	18.8	100
8VCRS	21.4	100
10VCRS	16.7	100
2VCRS 650	1.1	100
6VCRS 650	7.4	100
10VCRS 650	5.8	100

Reaction conditions—temperature: 60 °C; benzene: 33 mmol; acetonitrile: 191 mmol; H_2O_2: 88 mmol; time: 6 h.

increase in vanadia loading to 10 wt.% V_2O_5 causes a decline in phenol productivity. Catalysts calcined at 650 °C resulted in low conversion rate compared to catalysts calcined at 500 °C.

3.3. Discussion

Selective oxidation is believed to be working through a redox or Mars–van Krevelan mechanism with a rapid reoxidation of active sites by oxygen. Redox pairs Ce^{4+}/Ce^{3+} and V^{4+}/V^{5+} present in supported catalysts helps in this reaction to obtain highly selective conversion by rapid oxidation and reduction. In many studies concerning the mechanism involved in the catalytic reactions on vanadium oxide, the V=O species have been considered to play a significant role as active sites for the reactions [41]. Nomiya et al. summarized the requirement of one vanadium center acting in cooperation with the Mo(VI) atom for catalytic hydroxylation of benzene [42]. Vanadium containing mesoporous materials such as V-MCM-41 showed good catalytic activity for the oxidation of benzene over biocatalytic system with Pd-metal catalysts [43]. In complete benzene oxidation, the promoting effect of Pd and Ag over supported vanadium oxide has been related to the activation of oxygen on the metal particles, which enables the reverse oxidation of V^{4+} and leads to an equilibrium in the redox process [44]. Andreeva et al. studied titania, zirconia and ceria supported gold–vanadia catalysts for complete benzene oxidation and concluded that, the highest activity and stability was established for the ceria supported catalysts, which can be connected with high oxygen storage capacity of ceria. A strong synergistic effect is obtained between gold and vanadia on ceria thus being able to produce more active oxygen species [45].

In the present study, application of DR UV–vis and ^{51}V MAS-NMR shows that for low wt.% V_2O_5 loading, highly dispersed vanadia formed on the support, which consists tetrahedral V=O species while with increasing vanadia loading, formation of $CeVO_4$ evidenced. From ^{29}Si MASNMR studies, it is clear that silica is not forming any compounds with the supported vanadia and the solid-state reaction of ceria with vanadia is more favourable as the concentration of V_2O_5 increases. The catalysts exhibits NMR shifts corresponding to $CeVO_4$ and becomes highly symmetric as vanadium loading reaches to 10 wt.%. Thus, in 8VCRS, $CeVO_4$ observed along with dispersed sites while crystallization of this is found to be increased for 10VCRS. Catalysts exhibit catalytic performance in benzene oxidation according to changes in the structure. The high selectivity to phenol obtained on CRS supported catalysts is a consequence of the high dispersion of vanadium over the high surface area support. Upon high loading, the number of active surface sites decreases during the structural transformation from VO_x species on CeO_2 to $CeVO_4/CeO_2$ [39]. Thus, incipient formation of $CeVO_4$ does not significantly decrease the number of available surface VO_x sites, while an increase in the crystallization of the bulk $CeVO_4$ phase for high V_2O_5 loading results in a lower number of available surface VO_x sites, thus, decreasing total activity for 10 wt.% V_2O_5 loading while keeping high selectivity. This is in agreement with the instrumental characterization of the catalysts, which states only the presence of V^{5+} without any reduced vanadium centers and available lattice oxygen in Ce^{3+} makes redox mechanism to operate easily. Numerous studies also indicate that, for low vanadia loading, the V-surface species is an isolated VO_x monomer for silica supported catalysts contrary to titania and alumina [46]. Catalysts calcined at 650 °C, shows marginal decrease in activity attributed to the presence of bulk-like aggregates formed during the sintering of vanadium at high temperature calcination thus decrease the number of active sites available. However, presence of highly amorphous silica reduces the extent of sintering in the present case and crystallites formed only for 10 wt.% V_2O_5 loading corresponding to 11.25 at.% vanadium on the support. Thus, presence of high surface area amorphous rice husk silica as promoter for ceria helps high dispersion of active sites and the results of catalytic behaviour corresponding to the vanadia–support interaction.

3.4. Conclusion

Highly amorphous silica with high specific surface area could be prepared from an agrowaste rice husk and characterized using different techniques. Silica promoted ceria support material exhibits reasonably high surface area and high thermal stability at the calcination temperature. The combination of different physicohemical techniques used in this study revealed presence of different vanadium oxide species on the support. For low wt.% V_2O_5 loading, highly dispersed surface vanadia species evidenced on the support while that of $CeVO_4$ as loading approaches 10 wt.% corresponding to 11.25 at.% vanadium on the support. XRD and spectral characterization gives an impression that silica promoted ceria is an interesting carrier for the preparation of highly dispersed supported vanadia catalysts. Benzene oxidation activity shows that highly dispersed surface V=O species are responsible for the selective phenol formation by benzene oxidation while reduced number of these active sites due to $CeVO_4$ formation at high vanadia loading results decrease in conversion rate.

Acknowledgement

The authors thank SAIF, IITB, IISc, Bangalore for EPR and NMR analysis. R.T. gratefully acknowledge the help received from Shylesh, NCL, Pune.

References

[1] B.M. Reddy, A. Khan, Y. Yamada, T. Kobayashi, S. Loridant, J.C. Volta, J. Phys. Chem. B 106 (2002) 10964.
[2] M.A. Larrubia, G. Busca, Mater. Chem. Phys. 72 (2001) 337.
[3] Y.H. Kim, H.I. Lee, Bull. Korean Chem. Soc. 20 (1999) 1457.
[4] G.S. Wong, M.R. Concepcion, J.M. Vohs, J. Phys. Chem. B. 106 (2002) 6451.
[5] M.A. Larrubia, G. Busca, Mater. Chem. Phys. 72 (2001) 337–346.
[6] S. Sugunan, N.K. Renuka, A.R. Koshy, S.M. Varghese, C.G. Ramankutty, React. Kinet. Catal. Lett. 67 (2) (1999) 267.
[7] N. Ballarini, F. Cavani, M. Ferrari, R. Catani, U. Cornaro, J. Catal. 213 (2003) 95.
[8] X. Gao, J.M. Jehng, I.E. Wachs, J. Catal. 209 (2002) 43.
[9] M.L. Ferreira, M. Volpe, J. Mol. Catal. A: Chem. 184 (2002) 349.
[10] R. Neumann, M.L. Elad, Appl. Catal. A: Gen. 122 (1995) 85.
[11] M. Ponzi, C. Duschatzky, A. Carrascull, E. Ponzi, Appl. Catal. A: Gen. 169 (1998) 373.
[12] E.A. Aad, R. Bechara, J. Grimblot, A. Aboukais, Chem. Mater. 5 (1993) 793.
[13] J.M.D. Courcot, E.A. Aad, A. Aboukais, Chem. Mater. 14 (2002) 4118.
[14] G.S. Wong, J.M. Vohs, Surf. Sci. 498 (2002) 266.
[15] S. Chandrasekhar, K.G. Satyanarayana, P.N. Pramada, P. Raghavan, J. Mater. Sci. 38 (2003) 3159.
[16] N.Y. Alcin, V. Sevinc, Ceram. Int. 27 (2001) 219.
[17] C. Real, M.D. Alcala, J.M. Criado, J. Am. Ceram. Soc. 79 (8) (1996) 2012.
[18] F.W. Chang, M.S. Kuo, M.T. Tsay, M.C. Hsieh, Appl. Catal. A: Gen. 247 (2003) 309.
[19] F.W. Chang, M.T. Tsay, M.S. Kuo, C.M. Yang, Appl. Catal. A: Gen. 226 (2002) 213.
[20] F.W. Chang, W.Y. Kuo, H.C. Yang, Appl. Catal. A: Gen. 288 (2005) 53.
[21] F.W. Chang, W.Y. Kuo, K.C. Lee, Appl. Catal. A: Gen. 8517 (2003) 1.
[22] F.E. Massoth, Adv. Catal. 27 (1978) 265.
[23] F.M. Bautista, J.M. Campelo, A. Garcia, D. Luna, J.M. Marins, R.A. Quiros, A.A. Romero, Appl. Catal. A: Gen. 243 (2003) 93.
[24] Q. Fu, A. Weber, M.F. Stephanopoulos, Catal. Lett. 77 (1–3) (2001) 87.
[25] C. Real, M.D. Alcala, J.M. Criado, J. Am. Ceram. Soc. 79 (8) (1996) 2012.
[26] K. Sohlberg, S.T. Pantelides, S.J. Pennycook, J. Am. Chem. Soc. 123 (2001) 6609.
[27] J. Matta, D. Courcot, E.A. Aad, A. Aboukais, Chem. Mater. 14 (2002) 4118.
[28] M.V.M. Huerta, J.M. Coronado, M.F. Garcia, A.I. Juez, G. Deo, J.L.G. Fierro, M.A. Banares, J. Catal. 225 (1) (2004) 240.
[29] J. Matta, D. Courcot, E.A. Aad, A. Aboukais, J. Therm. Anal. Calorim. 66 (2001) 717.
[30] R. Cousin, M. Dourdin, E.A. Aad, D. Courcot, S. Capelle, M. Guelton, A. Aboukais, J. Chem. Soc., Faraday Trans. 93 (1997) 3863.
[31] D.R. Lide (Ed.), Handbook of Chemistry and Physics, 77 ed., CRS Press, Boca Raton, 1997.
[32] D.C.M. Dutiot, M. Schneider, P. Fabrizioli, A. Baiker, J. Mater. Chem. 7 (6) (1997) 271.
[33] G. Catana, R.R. Rao, B.M. Weckhuysen, P. van der Voort, E. Vansant, R.A. Scoonheydt, J. Phys. Chem. B 102 (1998) 8005.
[34] Z. Wu, H.S. Kim, P.C. Stair, S. Rugmini, S.D. Jackson, J. Phys. Chem. B 109 (2005) 2793.
[35] R. Cousin, S. Capelle, E.A. Aad, D. Courcot, A. Aboukais, Chem. Mater. 13 (2001) 3862.
[36] J.M. Vohs, T. Feng, G.S. Wong, Catal. Today 85 (2003) 303.
[37] X.S. Zhao, M.G.Q. Lu, C. Song, J. Mol. Catal. A: Chem. 191 (2003) 67.
[38] E.H. Park, M.H. Lee, J.R. Sohn, Bull. Korean Chem. Soc. 21 (9) (2000).
[39] B. Solsona, T. Blasco, J.M.L. Nieto, M.L. Pena, F. Rey, A.V. Moya, J. Catal. 203 (2001) 443.
[40] R. Cousin, D. Courcot, E.A. Aad, S. Capelle, J.P. Amoureux, M. Dourdin, A. Aboukais, Coll. Surf. A 158 (1999) 43.
[41] H. Kanzaki, T. Kitamura, R. Hamada, S. Nishiyama, S. Tsuruya, J. Mol. Catal. A: Chem. 208 (1–2) (2004) 203.
[42] K. Nomiya, K. Yagishita, Y. Nemoto, T. Kamataki, J. Mol. Catal. A: Chem. 126 (1997) 43.
[43] S.E. Park, J.W. Yoo, W.J. Lee, Proceedings of the 12th IZC, vol. II, Baltimore, USA, 1999, p. 1253.
[44] M. Vassileva, A. Andreeva, S. Dancheva, Appl. Catal. 69 (1991) 221.
[45] D. Andreeva, R. Nedyalkova, L. Ilieva, M.V. Abrashev, Appl. Catal. A: Gen. 246 (2003) 29.
[46] M.L. Ferreira, M. Volpe, J. Mol. Catal. A: Chem. 164 (2000) 281.